A Power Presizing Methodology for Electric Vehicle Traction Motors

Bekheira Tabbache, Sofiane Djebarri, Abdelaziz Kheloui, Mohamed Benbouzid

A Power Presizing Methodology for Electric Vehicle Traction Motors

Bekheira Tabbache[1,2], Sofiane Djebarri[2], Abdelaziz Kheloui[1] and Mohamed Benbouzid[2]

Abstract–*This paper proposes a methodology for presizing the power of an electric vehicle traction motor. Based on the vehicle desired performances, the electric motor optimal power can be calculated. The final objective is to meet the design constraints with minimum power under the European urban (ECE-15) and sub-urban (EUDC) driving cycles. The power presizing methodology is validated through extensive simulations for different induction motor-based electric vehicles.*

Keywords*: Electric vehicle, induction motor, power presizing, driving cycle.*

Nomenclature

EV = Electric Vehicle;
V = Vehicle speed;
V_b = Vehicle base speed;
V_{cr} = Vehicle cruising speed;
α = Grade angle;
P_v = Vehicle driving power;
F_w = Road load;
F_{ro} = Rolling resistance force;
F_{sf} = Stokes or viscous friction force;
F_{ad} = Aerodynamic drag force;
F_{cr} = Climbing and downgrade resistance force;
μ = Tire rolling resistance coefficient ($0.015 < \mu < 0.3$);
m = Vehicle mass;
g = Gravitational acceleration constant;
k_A = Stokes coefficient;
ξ = Air density;
C_w = Aerodynamic drag coefficient ($0.2 < C_w < 0.4$);
A_f = Vehicle frontal area;
V_0 = Head-wind velocity;
F = Tractive force;
k_m = Rotational inertia coefficient ($1.08 < k_m < 1.1$);
a = Vehicle acceleration;
J = Total inertia (rotor and load);
ω_m = Electric motor mechanical speed;
T_B = Load torque accounting for friction and windage;
T_L = Load torque;
T_m = Electric motor torque;
i = Transmission ratio;
η_t = Transmission efficiency;
R = Wheel radius;
J_V (J_W) = Shaft (wheel) inertia moment;
J_m = Electric motor inertia;
λ = Wheel slip;
N_m = Electric motor speed;
P_m = Electric motor power;
P_b = Base power.

I. Introduction

Recently, electric vehicles including fuel-cell and hybrid vehicles have been developed very rapidly as a solution to energy and environmental problems. From the point of view of control engineering, EVs have much attractive potential [1].

The shortcomings, which caused the EV to lose its early competitive edge, have not yet been totally overcome. Indeed, EVs have a low energy density and long charging time for the present batteries. Therefore, optimal energy management is very important in EVs; in addition, optimum design of the electric motor, selection of a proper drive, and optimal control strategy are the other major factors in EVs [2-8].

Selection of traction motors for the EV propulsion systems is a very important step that requires special attention. In fact, the automotive industry is still seeking for the most appropriate electric propulsion system. In this case, key features are efficiency, reliability and cost. The process of selecting the appropriate electric propulsion systems is however difficult and should be carried out at the system level. In fact, the choice of electric propulsion systems for EVs mainly depends on three factors: driver expectation, vehicle constraint, and energy source [11-13].

In this context, this paper proposes a methodology for presizing the electric motor propulsion power of an EV. The electric motor optimal power is therefore calculated regarding the EV desired performances and given driving cycles. The main objective behind is to find the electric motor minimum weight, volume, and cost that meet the design constraints with minimum power under the adopted driving cycles. The proposed power presizing methodology, which does not depend on the electric

motor type, is illustrated for an induction motor-based EV under the European urban (ECE-15) and sub-urban (EUDC) driving cycles.

II. EV Dynamic Analysis

This section derives the driving power to ensure the EV operation (Fig. 1) [6].

II.1. Road Load and Tractive Force

The road load consists of

$$F_w = F_{ro} + F_{sf} + F_{ad} + F_{cr} \tag{1}$$

The rolling resistance force F_{ro} is produced by the tire flattening at the roadway contact surface.

$$F_{ro} = \mu m g \cos\alpha \tag{2}$$

The rolling resistance force can be minimized by keeping the tires as much inflated as possible.

$$F_{sf} = k_A V \tag{3}$$

Aerodynamic drag, F_{ad}, is the viscous resistance of air acting upon the vehicle.

$$F_{ad} = \frac{1}{2}\xi C_w A_f (V + V_0)^2 \tag{4}$$

The climbing resistance (F_{cr} with positive operational sign) and the downgrade force (F_{cr} with negative operational sign) is given by

$$F_{cr} = \pm m g \sin\alpha \tag{5}$$

The tractive force in an electric vehicle is supplied by the electric motor in overcoming the road load. The equation of motion is given by

$$k_m m \frac{dV}{dt} = F - F_w \tag{6}$$

where $k_m = 1 + \dfrac{\eta_t i^2 J_m + 2J_w}{mR^2}$

The net force ($F - F_w$), accelerates the EV (or decelerates it when F_w exceeds F).

II.2. Electric Motor Ratings and Transmission

The power required to drive an EV has to compensate the road load F_w.

$$P_v = V F_w \tag{7}$$

The mechanical equation (in the motor referential) used to describe each wheel drive is expressed by

$$J \frac{d\omega_m}{dt} + T_B + T_L = T_m \tag{8}$$

The following equation is derived due to the use of a reduction gear.

$$\omega_{Wheel} = \frac{\omega_m}{i} \text{ and } T_{Wheel} = T_m i \eta_t \tag{9}$$

The load torque in the motor referential is given by.

$$T_L = \frac{T_{LWheel}}{i} = \frac{R}{i} F_w \tag{10}$$

The vehicle global inertia moment in the motor referential is given by

$$\begin{cases} J = J_W + J_V \\ J_V = \dfrac{1}{2} m \dfrac{R^2}{i^2}(1-\lambda) \end{cases} \tag{11}$$

III. Electric Motors for EVs

Major types of electric motors adopted or under consideration for electric vehicles include the dc motor, the induction motor, the permanent magnet synchronous motor, and the switched reluctance motor (Fig. 2) [7].

For EVs propulsion, the cage induction motor seems to be candidate that better fulfils their major requirements [7]. It has therefore been chosen to illustrate the proposed power presizing method. However, it should be noted that the pressing approach does not depend on the electric motor type.

Figure 3 shows the induction motor drive characteristics that should be dealt with when used as the EV propulsion [7], [13-14].

IV. Electric Motor Power Presizing

IV.1. Transmission Gear Ratio

The induction motor developed force on the EV driven wheels is expressed by

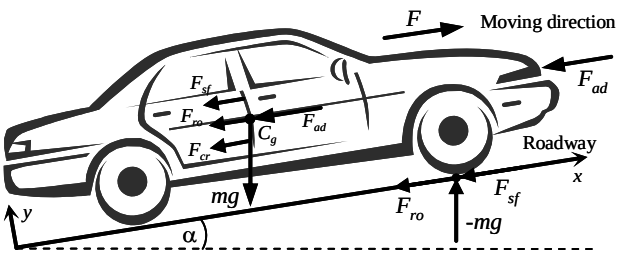

Fig. 1. Elementary forces acting on a vehicle.

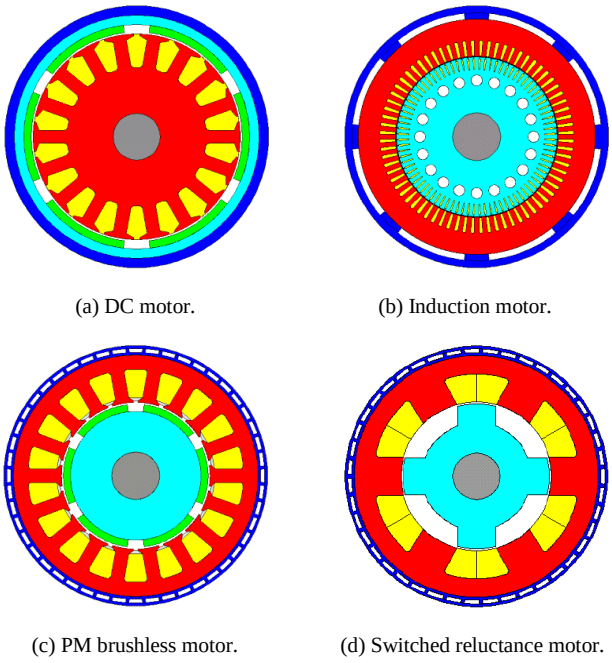

(a) DC motor. (b) Induction motor.

(c) PM brushless motor. (d) Switched reluctance motor.

Fig. 2. Electric motor types for EVs [7].

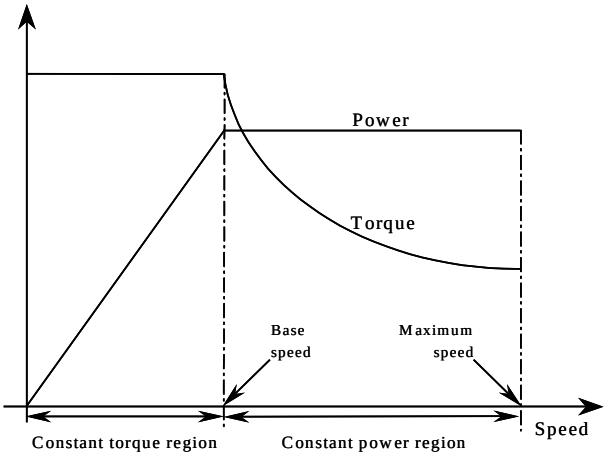

(a) Electric traction.

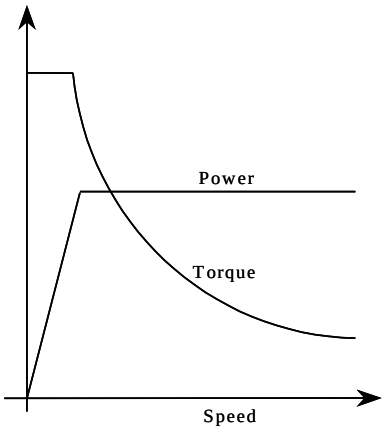

(b) Tractive effort versus speed.

Fig. 3. EV typical characteristics.

$$F = \eta_t \frac{iT_m}{R} \tag{12}$$

The transmission gear ratio i is designed such that the EV reaches its maximum speed at the induction motor maximum speed.

$$i = \frac{\pi N_{m\_max} R}{30 V_{max}} \tag{13}$$

A high value of this ratio has the advantage of allowing the use of high-speed motors which have a better power density, but with the disadvantage of more volume and then higher cost. A good compromise is generally not to exceed a value of $i = 10$ [12]. Moreover, if the induction motor has a wide constant power region, a single-gear transmission would be sufficient for a high-tractive force at low speeds.

IV.1. Induction Motor Power Presizing

Basic vehicle performance includes maximum cruising speed, gradeability, and acceleration. The induction motor power presizing is done for an EV whose data are given in the Appendix.

In this first presizing stage, the EV operation consists of three main segments: initial acceleration, cruising at the vehicle maximum speed and cruising at maximum gradeability.

1) Initial acceleration. The characteristic values of the EV force-speed profile, as illustrated by Fig. 4, are the base power, the base and the maximum speeds. The electric motor maximum speed must correspond to the vehicle maximum one.

In the case of initial acceleration, the induction motor power presizing is based on two steps: The first one is done under simplifying assumptions (null aerodynamic force). The second one takes into account all the EV resistance forces. The solution of (6) uses the base speed and the power found in the first step. The boundary conditions of (6) are: at $t = 0$, $V = 0$ and at $t = t_f$, $V = V_{cr}$.

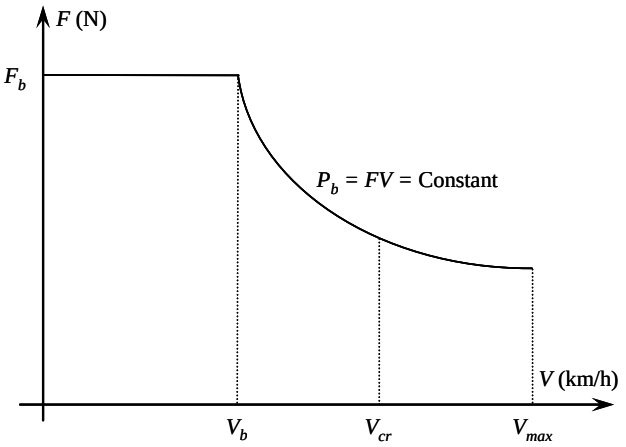

Fig. 4. EV force-speed profile.

Using (6), the EV acceleration time is defined by

$$t_a = \int_0^{V_f} \frac{k_1}{F - (k_2 V^2 + k_3)} dV \qquad (14)$$

where V_f is the final speed; k_1, k_2, and k_3 are constants values: $k_1 = k_m m$; $k_2 = 0.5\xi C_w A_f$; $k_3 = mg(\sin\alpha + \mu\cos\alpha)$. This expression can reformulated as

$$\frac{t_a}{\tau_b} = \frac{k_b^2}{\alpha_b - k_b} + \alpha_b log\left[\frac{\alpha_b - k_b}{\alpha_b - 1}\right] + k_b - 1 \qquad (15)$$

with $\alpha_b = \frac{P_b}{k_3 m g V_{cr}}$, $k_b = \frac{V_b}{V_{cr}}$, $\tau_b = \frac{k_m V_{cr}}{k_3 g}$.

The analytical solution of (15) is shown by Fig. 5.

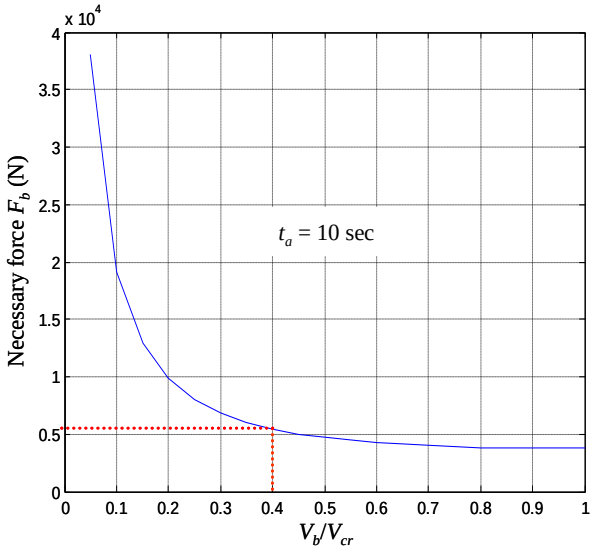

(a)

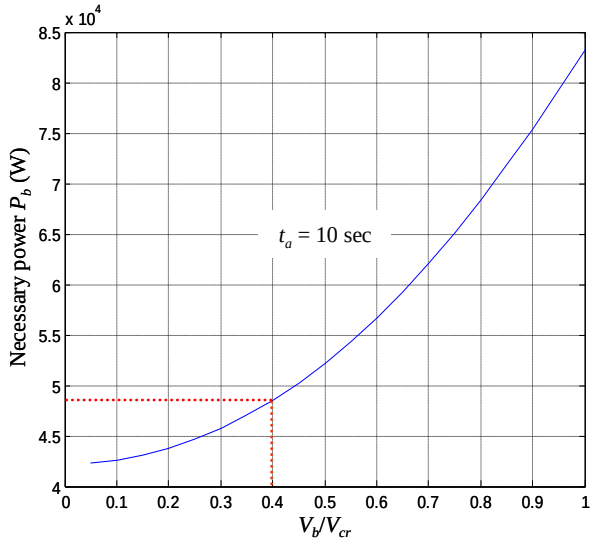

(b)

Fig. 5. Necessary force and power:
Acceleration from 0 to 80 km/h in 10 sec on ground level.

It illustrates the necessary power-speed profile for the EV initial acceleration in order to obtain the induction motor optimal power and base speed V_b which can be obtained so as

$$\frac{dF_b}{dt} = D_{max}$$

D_{max} is a compromise between the induction motor power and the acceleration force. In fact, D_{max} is chosen in order to minimize the power without a significant increase of the acceleration force.

Figure 5 shows that below $V_b = 0.4V_{cr}$, it is not interesting to decrease V_b because the necessary power does not greatly decrease. On the other hand, the acceleration force tends to considerably increase. This will lead to an increased propulsion motor size (the torque is an important dimensioning parameter in terms of size and weight). In this case, the first EV base parameters are the base speed ($V_b = 0.4V_{cr}$ = 32 km/h) and the base power (P_b = 48.53 kW).

Using these base values, the presizing second step consist in finding (6) numerical solution including all the resistance forces. In this case, the obtained initial acceleration time is larger than that specified in the desired performance. The correction of the base power and speed values are done using an iterative procedure combining analytical and numerical solutions. The new value is then: P_b = 54.86 kW, as illustrated by Fig. 6.

2) Cruising at vehicle maximum speed on ground level. To validate the base power and speed choices, it is mandatory to evaluate the induction motor power and torque in different operation modes and in particular at the vehicle maximum speed (V_{max}).

The power requirement to cruise at the EV maximum speed is given by

$$P_{V_{max}} = \frac{1}{2}\xi C_w A_f (V_{max} + V_0)^2 V_{max} + \mu m g V_{max} \qquad (16)$$

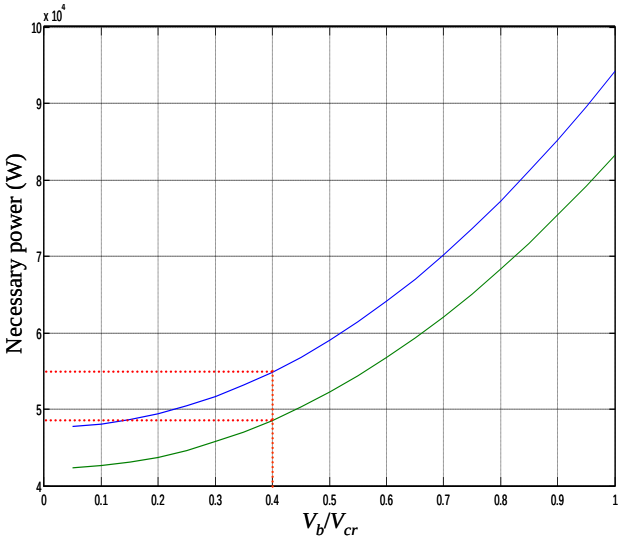

Fig. 6. Electric motor power: Step 1 (green) and step 2 (blue).

At V_{max}, the necessary power is about 22.18 kW. It is lower than the previous one found for initial acceleration. However, in case if the obtained power is greater, P_{Vmax} should be considered as the electric motor power rating.

3) Gradeability checking. The power found in the previous section is able to propel the EV at a regular highway speed (120 km/h) on a flat road. Using the induction motor torque and speed profiles, the necessary power on a 15% and 10% graded road can be evaluated.

Figure 7 indicates that the motor above calculated power of 54.86 kW can propel the EV at 76.80 km/h and 99.80 km/h on a 15% and 10% graded road, respectively.

V. Driving Cycles-Based Power Presizing

Another important consideration in the electric motor power presizing is the average power when driving with some typical stop-and-go driving patterns.

The average power can be obtained by

$$P_{average} = \frac{1}{T}\int_0^T \left(\frac{1}{2}\xi C_w A_f V^2 + \mu m g\right) V dt + \frac{1}{T}\int_0^T k_m m \frac{dV}{dt} dt \quad (17)$$

It is difficult to describe the road load and vehicle speed variations in all actual traffic environments accurately and quantitatively. However, some representative driving cycles have been developed to emulate typical traffic environments. Among them, the European Elementary urban cycle (ECE), the sub-urban cycle (EUDC) and sub-urban cycle for low-powered vehicles (EUDCL) (Fig. 8) [15].

Figure 8 shows then the EV electric motor necessary power in the case of European driving cycles with and without regenerative braking. Compared to the needed power shown in Fig. 9 ($P_{average}$ = 7.46 kW without regenerative braking and $P_{average}$ = 6.17 kW with regenerative braking), the optimal power found in the previous section is greater and can therefore meet the power requirement in these driving cycles.

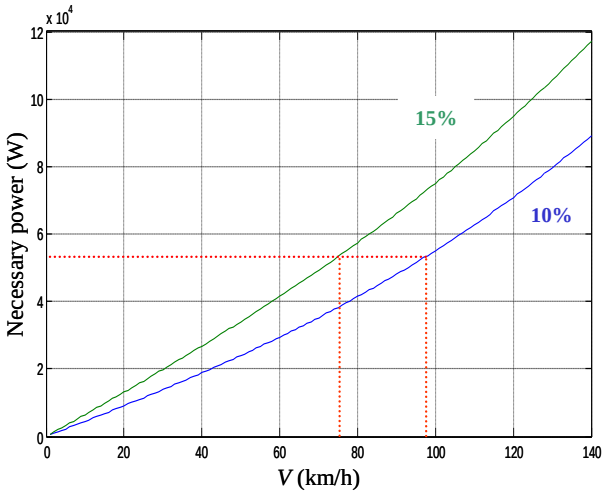

Fig. 7. The electric motor necessary power for gradeability.

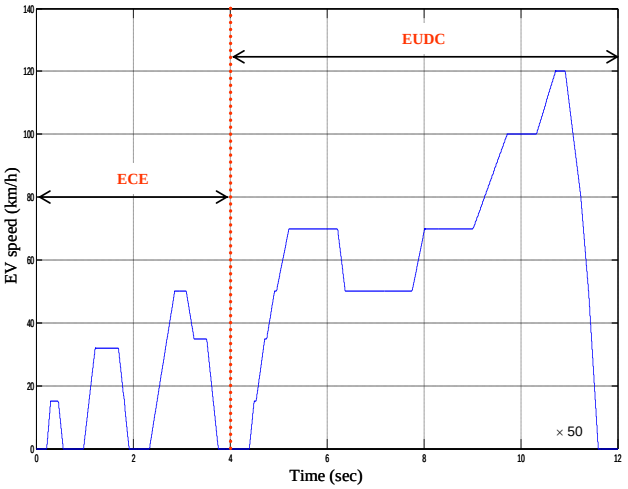

Fig. 8. The European ECE + EUDC driving cycle.

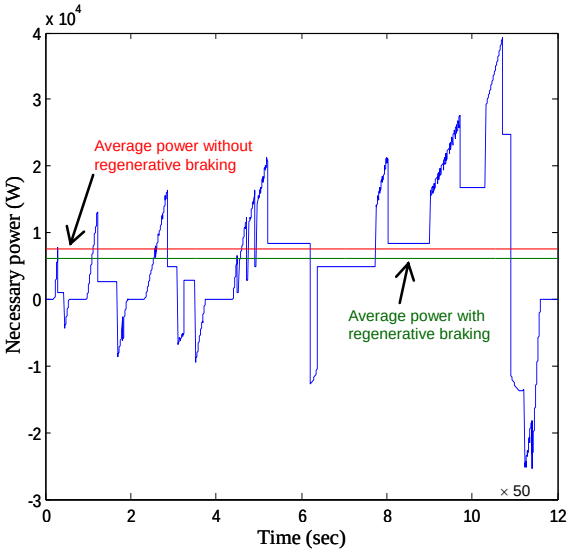

Fig. 9. Electric necessary power for the ECE + EUDC driving cycles.

For a comparative illustration, Table 1 show typical data for US well-know driving cycles; the FTP 75 urban and highway driving cycles [14].

The proposed power presizing methodology of an EV electric motor can finally be summarized in the flowchart shown by Fig. 10.

Table 1. Typical Data of Different Driving Cycles [14].

	V_{max} (km/h)	$V_{average}$ (km/h)	Average power full regenerative braking (kW)	Average power no regenerative braking (kW)
FTP 75 Urban	86.4	27.9	3.76	4.97
FTP 75 Highway	97.7	77.4	18.3	23.0
ECE-15	120	49.8	7.89	9.32

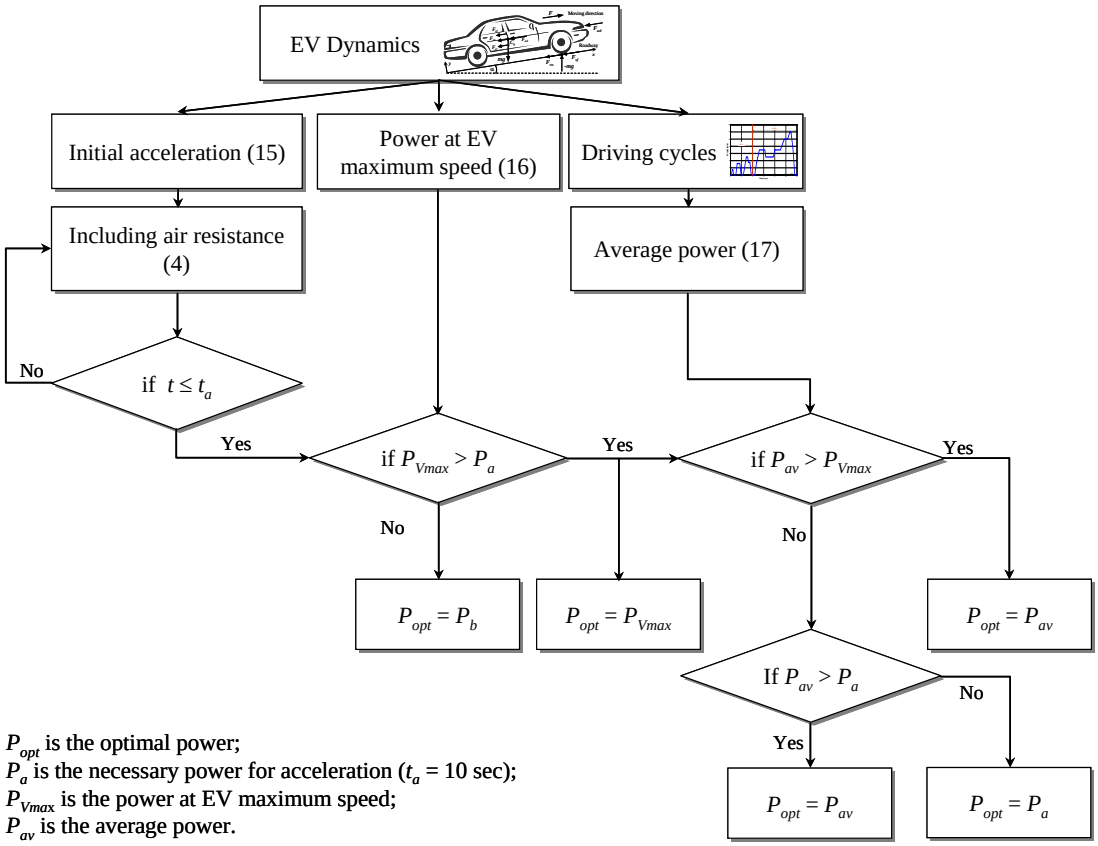

Fig. 10. Flowchart of the proposed power presizing methodology.

VI. EV Control Tests Using a Presized Induction Motor

The aim of this section is to check the induction motor-based EV performance under road load, especially the climbing resistance, and then choose the induction motor necessary power to propel the EV in normal driving cycles. For that purpose a sliding mode approach has been adopted to carry-out control tests on three induction motors for different graded road [16-18]. For that purpose, the acceleration and the corresponding time are defined by the European driving cycles illustrated by Fig. 8.

Simulations are carried-out on different induction motors with different power ratings. These simulations use the same above defined EV, whose parameters are given in Appendix. The main objective here is to find the minimum motor weight, volume and cost that will meet the design constraints with minimum power under the European ECE and EUDC driving cycles. After the average power calculation, the control uses standard motors: 15 kW, 37 kW and 75kW, whose rating are given in the Appendix. In this case the control is implemented in the extended constant power range.

The maximum gradeability of each motor is obtained by an iterative procedure using the EV model as indicated by Fig. 11. This Figure also shows necessary instantaneous and average powers to propel the EV.

For the validation of the obtained maximum gradeability, Fig. 12 illustrates the sliding mode control performances of the 37 kW induction motor-based EV including the 15.6% graded road. Figure 12a shows that very good speed tracking performances are achieved. Moreover, as clearly shown by the EV dynamics (Fig. 12.b), the developed torque variations are as large as are the variations of the accelerator pedal and the road profile.

The same control performances have also been achieved with the 15 and 75 kW induction motor-based EV: The obtained results clearly validate the proposed power presizing methodology.

VII. Conclusion

This paper has proposed a methodology for presizing the electric motor propulsion power of an EV. Indeed, the electric motor optimal power was calculated regarding the EV desired performances and given driving cycles; the European urban (ECE-15) and sub-urban (EUDC) driving cycles in our case. The main objective was to meet the design constraints with minimum power under the adopted driving cycles.

The power presizing methodology, which does not depend on the electric motor type, has been validated through extensive simulations for different induction motor-based EVs using a well-established advance control technique.

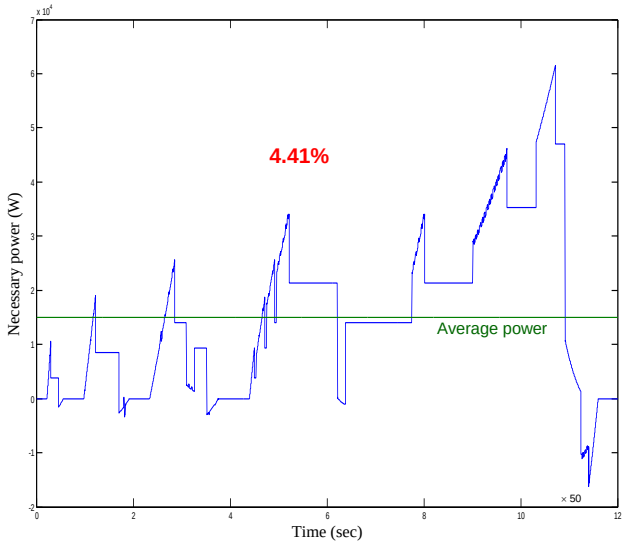

(a) 15 kW induction motor.

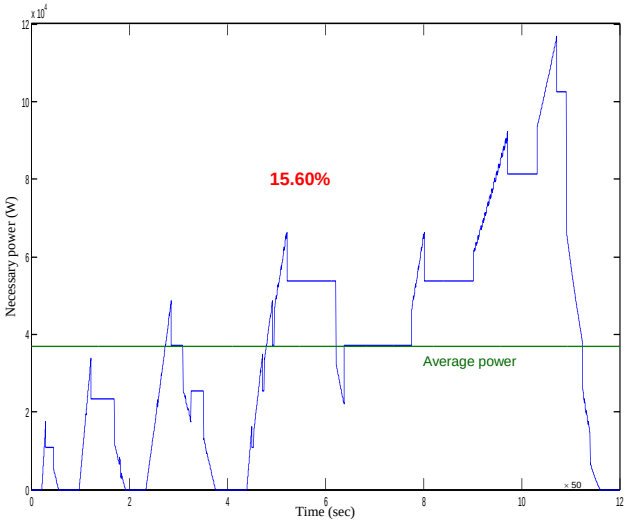

(b) 37 kW induction motor.

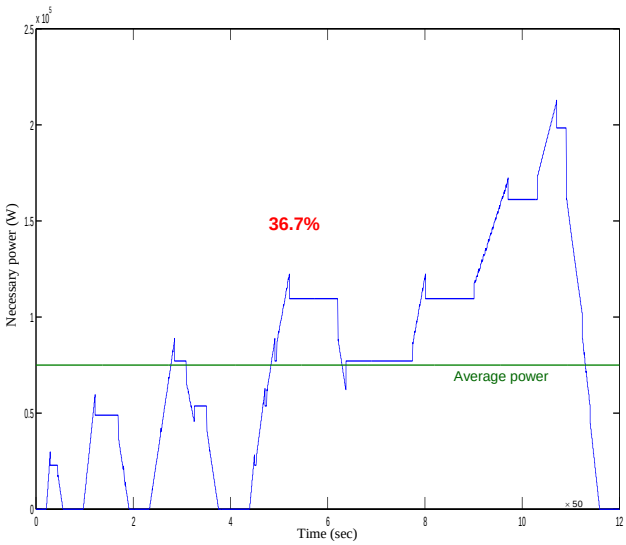

(c) 75 kW induction motor.

Fig. 11. Maximum gradeability and necessary powers.

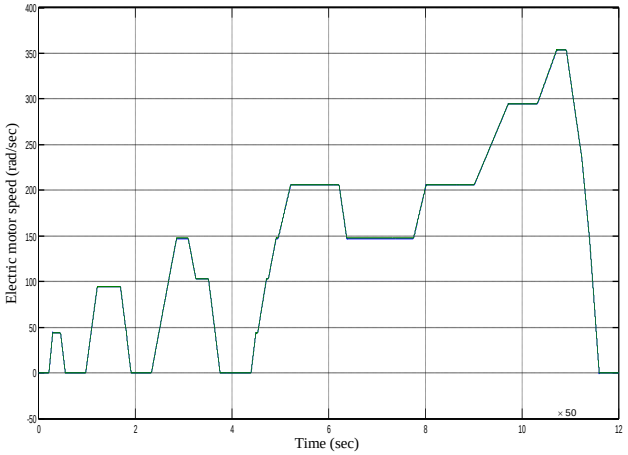

(a) Reference and the induction motor speed.

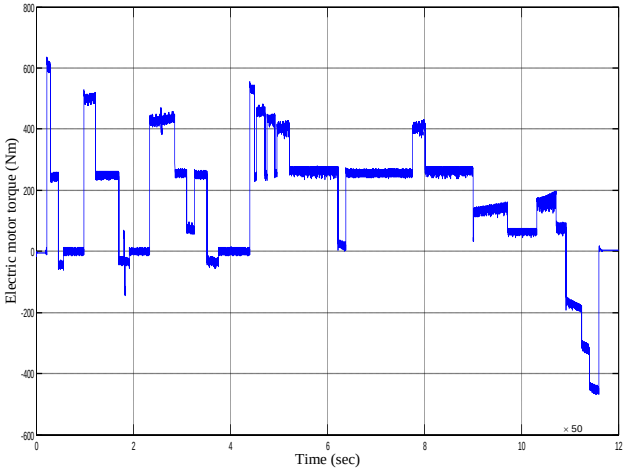

(b) The induction motor torque.

Fig. 12. The 37 kW induction motor-based EV control performances.

Appendix

Electric Vehicle Data

– Data: m = 1500 kg, μ = 0.015, C_w = 0.3, A_f = 2 m^2; R = 0.27 m, v_0 = 0;
– Acceleration: 0–80 km/h in 10 sec on ground level;
– Speeds: V_{max} = 120 km/h, N_{m_max} = 4000 rpm;
– Transmission: η_t = 90% (single-gear + differential)

Rated Data of the 15 kW Induction Motor

15 kW, 1480 rpm, p = 2
R_s = 0.2147 Ω, R_r = 0.2205 Ω
L_s = 0.065181 H, L_r = 0.065181 H, M = 0.0641 H
J = 0.102 kgm², k_f = 0.009541 Nms

Rated Data of the 37 kW Induction Motor

37 kW, 1480 rpm, p = 2
R_s = 0.0851 Ω, R_r = 0.0658 Ω
L_s = 0.0314 H, L_r = 0.0291 H, M = 0.0291 H,
J = 0.37kg.m², k_f = 0.02791Nmsec

Rated Data of the 75 kW Induction Motor

37 kW, 1480 rpm, $p = 2$
$R_s = 0.03552\Omega$, $R_r = 0.02092\Omega$
$L_s = 0.015435$ H, $L_r = 0.015435$ H, $M = 0.0151$ H
$J = 1.25$ kgm², $k_f = 0.03914$ Nmsec

References

[1] C.C. Chan, A. Bouscayrol and K. Chen, "Electric, hybrid, and fuel-cell vehicles: Architectures and modeling," *IEEE Trans. Vehicular Technology*, vol. 59, n°2, pp. 589-598, February 2010.

[2] X.D. Xue, K.W.E. Cheng, J.K. Lin, Z. Zhang, K.F. Luk, T.W. Ng and N.C. Cheung, "Optimal control method of motoring operation for SRM drives in electric vehicles," *IEEE Trans. Vehicular Technology*, vol. 59, n°3, pp. 1191-1204, March 2010.

[3] T.D. Batzel and K.Y. Lee, "Electric propulsion with the sensorless permanent magnet synchronous motor: model and approach," *IEEE Trans. Energy Conversion*, vol. 20, n°4, pp. 818-825, December 2005.

[4] C.T. Pan and J.H. Liaw, "A robust field-weakening control strategy for surface-mounted permanent-magnet motor drives," *IEEE Trans. Energy Conversion*, vol. 20, n°4, pp. 701-709, December 2005.

[5] S. Barsali, M. Ceraolo and A. Possenti, "Techniques to control the electricity generation in a series hybrid electrical vehicle," *IEEE Trans. Energy Conversion*, vol. 17, n°2, pp. 260-266, June 2002.

[6] B. Tabbache, A. Kheloui, M.E.H. Benbouzid, N. Henini, "SDTC-EKF control of an induction motor based electric vehicle," *International Review of Electrical Engineering*, vol. 5, n°3, pp. 1033-1039-432, June 2010.

[7] M. Zeraoulia, M.E.H. Benbouzid and D. Diallo, "Electric motor drive selection issues for HEV propulsion systems: A comparative study," *IEEE Trans. Vehicular Technology*, vol. 55, n°6, pp. 1756-1764, November 2006.

[8] B. Kou, L. Li, S. Cheng and F. Meng, "Operating control of efficiently generating induction motor for driving hybrid electric vehicle," *IEEE Trans. Magnetics*, vol. 41, n°1, Part. 2, pp. 488-491, January 2005.

[9] B.M. Baumann, G. Washington, B.C. Glennand and G. Rizzoni, "Mechatronic design and control of hybrid electric vehicles," *IEEE/ASME Trans. Mechatronics*, vol. 5, n°1, pp. 58-72, March 2000.

[10] G. Rizzoni, L. Guzzella and B.M. Baumann, "Unified modeling of hybrid electric vehicle drivetrains," *IEEE/ASME Trans. Mechatronics*, vol. 4, n°3, pp. 246-257, September 1999.

[11] B. Tabbache, A. Kheloui and M.E.H. Benbouzid, "Design and control of the induction motor propulsion of an electric vehicle," *in Proceedings of the IEEE VPPC'10*, Lille (France), pp. 1-6, September 2010.

[12] T. Hofman and C.H. Dai, "Energy efficiency analysis and comparison of transmission technologies for an electric vehicle," *in Proceedings of the IEEE VPPC'10*, Lille (France), pp. 1-6, September 2010.

[13] T. Wang, P. Zheng, Q. Zhang and S. Cheng, "Design characteristics of the induction motor used for hybrid electric vehicle," *IEEE Trans. Magnetics*, vol. 41, n°1, Part. 2, pp. 505-508, January 2005.

[14] M. Ehsani, Y. Gao, and A. Emadi, *Modern Electric, Hybrid Electric, and Fuel Cell Vehicles*: Fundamentals, Theory, and Design, CRC Press, 2009.

[15] A. Froberg and L. Nielsen, "Efficient drive cycle simulation," *IEEE Trans. Vehicular Technology*, vol. 57, n°3, pp. 1442-1453, May 2008.

[16] Y. Wang, X. Zhang, X. Yuan, and G. Liu, "Position-sensorless hybrid sliding-mode control of electric vehicles with brushless DC motor," *IEEE Trans. Vehicular Technology*, vol. 60, n°2, pp. 421-432, February 2011.

[17] M.E.H. Benbouzid, D. Diallo and M. Zeraoulia, "Advanced fault-tolerant control of induction-motor drives for EV/HEV traction applications: From conventional to modern and intelligent control techniques," *IEEE Trans. Vehicular Technology*, vol. 56, n°2, pp. 519-528, March 2007.

[18] A.B. Proca, A. Keyhani and J.M. Miller, "Sensorless sliding-mode control of induction motors using operating condition dependent models," *IEEE Trans. Energy Conversion*, vol. 18, n°2, pp. 205-212, June 2003.

[1]Ecole Militaire Polytechnique, UER ELT, 16111 Algiers, Algeria.
[2]University of Brest, EA 4325 LBMS, Rue de Kergoat, CS 93837, 29238 Brest Cedex 03, France (e-mail: Mohamed.Benbouzid@univ-brest.fr).

Bekheira Tabbache was born in Chlef, Algeria in 1979. He received the B.Sc. and the M.Sc. degrees in electrical engineering, from the Polytechnic Military Academy, Algiers, Algeria, in 2003 and 2007 respectively. He is currently working toward the Ph.D. degree in electric vehicle fault-tolerant control with the University of Brest, Brest, France.

In 2004, he joined the Electrical Engineering Department of the Polytechnic Military Academy, Algiers, Algeria as a Teaching Assistant.

Sofiane Djebarri was born in Algeria in 1984. He received the B.Sc and M.Sc. degrees in electrical engineering, from the National Polytechnic School, Algiers, Algeria, and the University of Paris-Sud 11, France, in 2009 and 2010 respectively. He is a Teaching and Research assistant at the French Naval Academy since September 2010.

He is currently pursuing Ph.D. studies on electrical machines design for renewable energy applications in collaboration with the University of Brest.

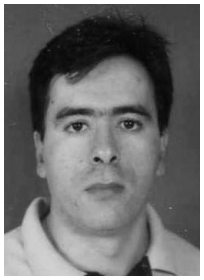

Abdelaziz Kheloui received the M.Sc. degree in Electrical Engineering from the Ecole Nationale d'Ingénieurs et Techniciens of Algeria (ENITA), Algiers, Algeria in 1990 and the Ph.D. degree also in electrical engineering from the National Polytechnic Institute of Lorraine, Nancy, France in 1994. Since 1994 he has been an Associate than a Full Professor at the Electrical Engineering Department of the Polytechnic Military Academy, Algiers, Algeria.

His current research interests are control of electrical drives and power electronics.

Mohamed El Hachemi Benbouzid (S'92–M'95–SM'98) was born in Batna, Algeria, in 1968. He received the B.Sc. degree in electrical engineering from the University of Batna, Batna, Algeria, in 1990, the M.Sc. and Ph.D. degrees in electrical and computer engineering from the National Polytechnic Institute of Grenoble, Grenoble, France, in 1991 and 1994, respectively, and the Habilitation à Diriger des Recherches degree from the University of Picardie "Jules Verne," Amiens, France, in 2000.

After receiving the Ph.D. degree, he joined the Professional Institute of Amiens, University of Picardie "Jules Verne," where he was an Associate Professor of electrical and computer engineering. In September 2004, he joined the University Institute of Technology (IUT) of Brest, University of Brest, Brest, France, as a Professor of electrical engineering. His main research interests and experience include analysis, design, and control of electric machines, variable-speed drives for traction, propulsion, and renewable energy applications, and fault diagnosis of electric machines.